



HAL
open science

Biostratigraphy and Paleoenvironmental significance of Paleogene foraminiferal assemblages from Dashte Zari area in High Zagros, west Iran

Seyed Ahmad Babazadeh, Dominique Cluzel

► **To cite this version:**

Seyed Ahmad Babazadeh, Dominique Cluzel. Biostratigraphy and Paleoenvironmental significance of Paleogene foraminiferal assemblages from Dashte Zari area in High Zagros, west Iran. *Brazilian Journal of Geology*, In press. hal-03773390

HAL Id: hal-03773390

<https://hal.science/hal-03773390>

Submitted on 9 Sep 2022

HAL is a multi-disciplinary open access archive for the deposit and dissemination of scientific research documents, whether they are published or not. The documents may come from teaching and research institutions in France or abroad, or from public or private research centers.

L'archive ouverte pluridisciplinaire **HAL**, est destinée au dépôt et à la diffusion de documents scientifiques de niveau recherche, publiés ou non, émanant des établissements d'enseignement et de recherche français ou étrangers, des laboratoires publics ou privés.

1 **Biostratigraphy and Paleoenvironmental significance of Paleogene foraminiferal**
2 **assemblages from Dashte Zari area in High Zagros, west Iran**

3 Seyed Ahmad Babazadeh^{1*} and Dominique Cluzel²

4 1- Department of Sciences, Payame Noor University, Po. Box 19395-3697, Tehran, Iran

5 2 - Institut de Sciences Exactes et Appliquées, Université de la Nouvelle-Calédonie, BP R4,
6 98851 Noumea Cedex, New Caledonia

7 * Corresponding author, e-mail:seyedbabazadeh@yahoo.com

8

9 **Abstract**

10 The Paleogene carbonate deposits of Pabdeh and Jahrum formations are widespread in the
11 northwest of the Shahrekord region (Dashte Zari area) in the High Zagros Mountains of Iran and
12 record lateral and upward transition from open marine into shallow water environment within the
13 Zagros foreland basin. The Pabdeh Formation shows a succession of open marine pelagic and
14 hemipelagic limestone, argillaceous limestone, and argillaceous chert. It consists of planktonic
15 wackestone, pellet-planktonic wackestone, mudstone with planktonic foraminifera, and
16 radiolarian siliceous wackestone. The planktonic foraminifera are assigned to the Late Paleocene
17 to Late Eocene, and correspond to subtropical to tropical Zones P4b–E15. Only one planktonic
18 biozone (Zone E12), which corresponds to the high level stand of the Bartonian climate optimum
19 (MECO) was not recognized in likely response to a tectonic event. The Jahrum Formation is
20 represented by bioclast-bearing limestone and calcarenite. It consists of benthic foraminiferal
21 wackestone, benthic foraminiferal-red algal packstone, and bioclast-intraclast packstone

22 deposited in a shallow platform environment. The Jahrum Formation is inter-fingered in the
23 upper part of the Pabdeh Formation and finally overlies it conformably during the Bartonian-
24 Priabonian. Shallowing and offlap relationships record basin shrinking, while repeated inter-
25 fingering signals moderate tectonic subsidence. Both formations are disconformably covered by
26 the Late Oligocene-Miocene Asmari Formation.

27 **Keywords**

28 Biostratigraphy, Dashte Zari, Pabdeh and Jahrum formations, Zagros foreland basin, Paleogene
29 foraminifera, West Iran

30

31 **1. INTRODUCTION**

32 The Iranian ranges long have been considered part of the Alpine-Himalayan System (Stöcklin,
33 1968, 1977, Sengör *et al.*, 1988, Babazadeh, 2003). This orogenic belt, which resulted from the
34 closure of the Mesozoic Neo-Tethys, extends from western Europe (west Neo-Tethys) to Tibet
35 passing through Turkey, Iran, Afghanistan (central Neo-Tethys), and possibly continues to
36 Burma and Indonesia (east Neo-Tethys) (Sengör *et al.* 1988; Ahmad *et al.*, 2014) (Fig. 1A).
37 Multiple continental blocks were amalgamated and are now separated by ophiolitic complexes
38 (Stöcklin, 1977). During the Late Cretaceous, northeastward subduction beneath the Iranian sub-
39 plate led to the closure of the central Neo-Tethys and ophiolite obduction onto the margin of the
40 Afro-Arabian Plate (Stöcklin, 1977; Berberian & King, 1981; Davoodzadeh & Schmidt, 1981;
41 Stoneley, 1981; Berberian, 1995; Alavi, 2004). Continent-continent collision starting in the
42 Cenozoic led to the formation of the Zagros fold-and-thrust belt and associated Zagros foreland
43 basin, in which Late Cretaceous to Miocene sediments accumulated (Fig. 1B). During the

44 Paleocene and Eocene, the Pabdeh Formation (pelagic marls and argillaceous limestones) and
45 the Jahrum Formation (shallow marine carbonates) were deposited in the middle part and on both
46 sides of the Zagros basin axis respectively (Motiei, 1993). During the Oligocene–Miocene this
47 basin narrowed gradually and the Asmari Formation, which consists of dolomitized carbonate
48 ramp limestones, calcareous sandstones and evaporites was deposited (e.g. Ehrenberg et al.,
49 2007).

50 In the study area the lower contact of the Pabdeh Formation with the underlying Upper
51 Cretaceous Gurpi Formation is faulted. The Jahrum Formation is inter-fingered in the upper part
52 of Pabdeh Formation and overlaps it at his top. In the southwestern part of the Zagros basin, the
53 Asmari Formation overlies the Pabdeh Formation, whereas in the Fars and Lurestan regions it
54 covers the Jahrum and Shahbazan formations. Although the lower part of the Asmari Formation
55 is locally interfingered with the Pabdeh Formation, its upper part extends over the entire Zagros
56 basin. The Zagros Mountains include the High Zagros (Internal Zagros), Folded Zagros (Outer
57 Zagros), and Khuzestan plain. In the High Zagros, the Shahrekord region of Chahar-Mahale
58 Bakhtiari Province is subdivided into northeast (Z1), central (Z2), and southwest (Z3) fault-
59 bounded zones. The Central Zone (Z2) is located between the Saman - Fereidoon Shahr thrust
60 (F1) and the Bazoft thrust (F3) (Zahedi & Rahmati Ilkhechi, 2006). This zone is divided into two
61 smaller sub-zones Z2a and Z2b, which are located in the Shahrekord region (Fig. 2A). It consists
62 of the Upper Cretaceous to Paleogene Gurpi, Jahrum, Pabdeh, and Asmari formations. The
63 studied Dashte Zari section (32°25'N; 50°20'E) is located in the sub-zone Z2b of the structural
64 division of northwest Shahrekord city (Fig. 2B).

65

66 In the study area, the Pabdeh Formation is subdivided into Lower and Upper units and consists
67 of pelagic carbonate and siliceous sediments, which include a succession of gray thin-bedded
68 limestone, cream argillaceous limestone, and argillaceous chert. In contrast, the Jahrum
69 Formation is composed of shallow marine grey to cream bioclastic limestone and calcarenite
70 (Fig. 3A).

71 James & Wynd (1965) and Adams & Bourgeois (1967) were pioneers in the study of
72 microfossils and microfacies of the Paleogene carbonate deposits in Zagros basin. They
73 established the benthic foraminiferal biozonation of the Jahrum Formation in southwest and west
74 Iran. Basic works on the Paleogene biostratigraphy of benthic foraminifera in the High Zagros
75 Basin and other basins along the southwestern margin of Iran focused mostly on microfacies and
76 macrofossils (Rahghi, 1976, 1978, 1980, 1983; Kalantari, 1976, 1978, 1980, 1986; Stöcklin &
77 Setudehnia, 1991; Khatibi Mehr & Moalemi, 2009; Babazadeh *et al.*, 2015). The foraminiferal
78 assemblage zones of Jahrum Formation and its equivalents were reported by a few researchers
79 such as James & Wynd (1965) and Hottinger (2007) On the other hand, the Pabdeh Formation
80 was analyzed by several researchers (Kalantari, 1986; Babazadeh *et al.*, 2010; Daneshian *et al.*,
81 2015; Chegini *et al.*, 2016; Moradian & Baghbani, 2016; Moradian *et al.*, 2017; Hadavandkhani
82 *et al.*, 2018) based on biofacies and stratigraphy of samples from outcrops of the folded Zagros
83 and Khuzestan plain, whereas the analysis of biostratigraphic zonation of planktonic foraminifera
84 are extensively conducted for the first time in the High Zagros of Chahar- Mahale Bakhtiari
85 Province. The purpose of this study is: 1) to document the planktonic and benthic foraminiferal
86 fauna, and 2) to introduce the Paleogene foraminiferal biozonations.

87

88

89

90

91 **2. MATERIALS AND METHODS**

92 A total of 111 samples of Pabdeh and Jahrum formations from the Dashte Zari section are used
93 in this study. Most of the diagnostic criteria such as the size of the test, the shape of chambers,
94 the thickness of the test, and the number of keels can be recognized in axial and sub-axial
95 sections in thin sections. The thin sections of the specimen samples were prepared in Payame
96 Noor University Laboratory. The Paleogene planktonic zonations were established by many
97 researchers: Toumarkine & Lutertacher (1985); Berggren *et al.* (1995); Olsson *et al.* (1999);
98 Berggren & Pearson (2005), and Wade *et al.* (2011). Besides, the calibration of the first
99 occurrence (FO) and last occurrence (LO) data of planktonic species is based on Berggren *et al.*
100 (1995); and Berggren & Pearson (2005). The identification of Paleogene planktonic
101 foraminiferal species in thin sections is carried out based on the following publications: Postuma
102 (1971); Wernli *et al.* (1997); Konijnenburg *et al.* (1998); Premoli Silva *et al.* (2003); Babazadeh
103 *et al.* (2010); Daneshian *et al.* (2015); Sarigul *et al.* (2017), and Sari (2017) The species
104 identification of benthic foraminifera was made by reference mainly to Ellis & Messina (1940);
105 Le Calvez (1949); Cole & Gravell (1952); Hanzawa (1957); Rahaghi (1980); Loeblich & Tappan
106 (1987); Ozgen (2000); Sirel (2003, 2009); Hottinger (2007); Serra-Kiel *et al.* (2016), and
107 Hayward *et al.* (2021). The biozonal schemes of Berggren *et al.* (1995) and Berggren & Pearson
108 (2005) were correlated with relevant data levels of species found in the study area (Figs. 4A &
109 4B).

110

111 **3. STRATIGRAPHY**

112 The excellent exposures of Paleogene carbonate sedimentary rocks of the High Zagros basin of
113 southwest and west Iran have allowed detailed stratigraphical and micropaleontological
114 investigations of these rocks. The Paleocene-Eocene marine deposits of the Pabdeh and Jahrum
115 formations in the Dashte Zari section contain planktonic and larger benthic foraminifera, which
116 provide the basis for regional biostratigraphy. Due to the presence of faults and discontinuous
117 outcrops of Paleogene successions in the Shahrekord region, the planktonic biostratigraphic
118 research was not conducted until today.

119

120 **3.1. BIOSTRATIGRAPHY**

121 The planktonic foraminiferal zonations of Berggren *et al.* (195); Berggren & Pearson (2005) and
122 Wade *et al.* (2011), and the benthic foraminiferal zonations of Serra-Kiel *et al.* (1998) and
123 Hottinger (2007) are adopted for comparison and interpretation. However, a brief evaluation of
124 the depositional setting is also explained in terms of Murray (1991), Hottinger (1983, 1997), and
125 Flugel (1982, 2004). The planktonic and benthic foraminiferal assemblages from hemipelagic
126 and neritic successions of the High Zagros provide the first published biostratigraphic data on
127 this area. A total of 46 planktonic foraminiferal species belonging to 14 different genera, and 19
128 benthic foraminiferal species belonging to 17 different genera have been identified and led to the
129 recognition of 14 planktonic biozones and 3 benthic associations respectively. The columnar
130 stratigraphic sections are summarized in figures 5 and 6, which show the distribution of selected
131 taxa of planktonic and benthic foraminifera. The micrographs of thin sections of Paleogene
132 planktonic and benthic foraminiferal species are shown in plates 1-4 and plate 5 respectively.
133 The planktonic foraminiferal biozonations enable to correlate with other biostratigraphic scales
134 and to make more precise their age determination (Fig. 7).

135

136 **Pabdeh Formation**

137 The planktonic foraminiferal biozones are as follows:

138 **Pp1 - *Acarinina subsphaerica* Zone (TRZ)**

139 **TRZ: Total Range Zone**

140 Estimated age: 59.2–56.5 Ma (Cande & Kent, 1965) ; 60.0– 57.3 Ma (Luterbacher *et al.*, 2004 ;
141 Middle-Late Paleocene (Wade *et al.*, 2011).

142 This zone, characterized by the total range zone of *Acarinina subsphaerica* (Subbotina) has a
143 thickness of 9 meters (bed Pl 1 to bed Pl 7) (Fig. 5). It is equivalent to subzone P4a
144 (*Globanomalina pseudomenardii-Acarinina subsphaerica* CRSZ), subzone P4b (*Ac.*
145 *Subsphaerica-Ac. Soldadensis* ISZ) of Berggren *et al.* (1995), and subzone P4b (*Ac.*
146 *Subsphaerica* PRSZ) of Berggren & Pearson (2005) and Wade *et al.* (2011), thereby indicating
147 Selandian to Thanetian age for the lowermost part of the Pabdeh Formation in the study area.
148 The associated planktonic fauna is *Acarinina decepta* (Martin), *Acarinina mckannai* (White), and
149 *Acarinina cf. nitida* (Martin). The associated foraminiferal taxa are well represented throughout
150 the Late Paleocene to Early Eocene. This zone is assigned to the Late Selandian-Thanetian in the
151 study area.

152 **Pp2-*Morozovella velascoensis* Zone (PRZ)**

153 **PRZ: Partial Range Zone**

154 Estimated age: 55.9–55.5 Ma (Cande & Kent, 1995); 56.7– 55.8 Ma (Luterbacher *et al.*, 2004);
155 late Paleocene (Wade *et al.*, 2011).

156 Biostratigraphic interval characterized by the partial range of the nominate taxon between the LO
157 (Last Occurrence) of *Acarinina mckannai* (White) and the first occurrence (FO) of *Morozovella*
158 *marginodentata* (Subbotina). This zone has a thickness of 3.5 meters and only appears on
159 horizon Pl 8 (Fig. 5). It is comparable to Zone P4c (*Ac. soldadoensis*-*Gl. pseudomenardii* ISZ);
160 Zone P5 (*M. velascoensis* IZ) of Berggren *et al.* (1995) and subzone P4c (*Ac. soldadoensis*-*Gl.*
161 *pseudomenardi* CRSZ), Zone P5 (*M. velascoensis* IZ), Zone E1 (*A. sibiyaensis* LOZ) and Zone
162 E2 (*P. wilcoxensis*-*M. velascoensis* CRZ) of Berggren & Pearson (2005), thereby indicating Late
163 Paleocene (Thanetian) to Early Eocene age in this study. This zone also contains *Acarinina*
164 *nitida* (Martin).

165

166 **Pp3- *Morozovella marginodentata*- *Morozovella formosa* Zone (IZ)**

167 **IZ: Interval Zone**

168 Estimated age: 54.5–54.0 Ma (Cande & Kent, 1995); 54.9– 54.4 Ma (Luterbacher *et al.*, 2004);
169 Early Eocene (Early Ypresian) (Wade *et al.*, 2011).

170 This zone, marked by the FO of *Morozovella marginodentata* (Subbotina) and the FO of
171 *Morozovella formosa* (Bolli), extends over a thickness of 2.5 meters (bed Pl 9 to bed Pl 10) (Fig.
172 5). It corresponds to the *Globorotalia edgari* Zone of Premoli Silva & Bolli, (1973) (in part), the
173 Zone P6a (*Morozovella velascoensis*- *M. formosa*/ *M. lensiformis* ISZ) of Berggren *et al.* (1995),
174 and the Zone E3 (*Morozovella marginodentata* PRZ) of Berggren & Pearson (2005) and Wade *et*
175 *al.* (2011). The associated planktonic foraminifera of this biozone are *Morozovella edgari*
176 (Premoli Silva & Bolli), *Morozovella velascoensis* (Cushman), *Morozovella acuta* (Toulmin),
177 *Morozovella marginodentata* (Subbotina) and *Acarinina nitida* (Martin). The stratigraphic range
178 of this zone is Early Eocene (Early Ypresian).

179 **Pp4- *Morozovella formosa* - *Guembeltrioides lozanoi* Zone (IZ)**

180 Estimated age: 54.0–52.3 Ma (Cande & Kent, 1995); 54.4– 52.3 Ma (Luterbacher *et al.*, 2004);

181 Early Eocene (Ypresian) (Wade *et al.*, 2011).

182 The biostratigraphic interval is characterized by the FO of *Morozovella formosa* (Bolli) and FO

183 of *Guembeltrioides lozanoi* (Colom). This zone is 5 meters thick (bed Pl 10 to bed Pl 14) (Fig.

184 5). It corresponds to the Zone P6b (*M. aragonensis*- *M. formosa*) of Berggren *et al.* (1995) and

185 Zone E4 (*Morozovella formosa* LOZ) of Berggren and Pearson (2005) and Wade *et al.* (2011).

186 The associated planktonic foraminifera of this biozone are *Acarinina cf. nitida* (Martin), *Igorina*

187 (*Pearsonites*) *broedermanni* (Cushman & Bermudez), *Morozovella velascoensis* (Cushman),

188 *Morozovella marginodentata* (Subbotina), and *Morozovella subbotinae* (Morozova). This

189 associated species ranges within the Early Eocene (Ypresian) age.

190

191 **Pp5- *Guembeltrioides lozanoi* - *Acarinina pentacamerata* (IZ)**

192 Estimated age: 52.3–50.8 Ma (Cande & Kent, 1995 and Luterbacher *et al.*, 2004); Early Eocene

193 (Ypresian) (Wade *et al.*, 2011).

194 This zone, characterized by the FO of *Guembeltrioides lozanoi* (Colom) and the FO of

195 *Acarinina pentacamerata* (Subbotina), extends over a thickness of 2.8 meters (Pl 14 to Pl 18)

196 (Fig. 5). This biozone can be equivalent to the Zone P7 (*M. aragonensis*/ *M. formosa*) and Zone

197 E5 (*M. aragonensis*/ *M. subbotinae* CRZ) of Berggren & Pearson (2005) and Wade *et al.* (2011).

198 The associated fauna of this biozone consists of *Igorina broedermanni* (Cushman and

199 Bermudez), *Morozovella subbotinae* (Morozova), *Guembeltrioides lozanoi* (Colom), and

200 Radiolaria and extends throughout the Early Eocene (Ypresian).

201 **Remark:** the first radiolarian association occurs in the interval from bed 12 to bed 18 (Fig. 5).

202

203 **Pp6- *Acarinina pentacamerata* - *Planorotalites palmerae* Zone (IZ)**

204 Estimated age: 50.8–50.4 Ma (Cande & Kent, 1995); 50.8– 50.3 Ma (Luterbacher *et al.*, 2004);

205 Early Eocene (Ypresian) (Wade *et al.*, 2011).

206 This zone, marked by the FO of *Acarinina pentacamerata* (Subbotina) and the FO of

207 *Planorotalites palmerae* Cushman and Bermudez, is 2.5 meters thick (bed Pl 18 to bed Pl 20)

208 (Fig. 5). It is equivalent to Zone P8 (*M. aragonensis* PRZ) of Berggren *et al.* (1995) and Zone E6

209 (*A. pentacamerata* PRZ) of Berggren & Pearson (2005) and Wade *et al.* (2011). This zone also

210 contains *Guembeltrioides lozanoi* (Colom) and *Turborotalia prolata* (Belfoed). The

211 stratigraphic range of this zone is assigned to the Early Eocene (Early Ypresian).

212

213 **Pp7- *Planorotalites palmerae* - *Guembeltrioides nuttalli* Zone (IZ)**

214 *Guembeltrioides nuttalli* is synonymous with *Globigerinoides higginsi*

215 Estimated age: 50.4–49.0 Ma (Cande & Kent, 1995); 50.3– 48.6 Ma (Luterbacher *et al.*, 2004);

216 Early Eocene (Late Ypresian) (Wade *et al.*, 2011).

217 This zone, characterized by the FO of *Planorotalites palmerae* Cushman and Bermudez and the

218 FO of *Guembeltrioides nuttalli* (Hamilton), is 2.3 meters thick (bed Pl 20 to bed Pl 22) (Fig. 5).

219 It corresponds to the Zone P9 (*P. palmerae* – *G. nuttalli* IZ) of Berggren *et al.* (1995); Zone E7

220 (*Acarinina cuneicamerata* LOZ) of Berggren & Pearson (2005) and Zone E7a (*Acarinina*

221 *cuneicamerata* LOSZ) of Wade *et al.* (2011). This zone also contains *Acarinina collectea*

222 (Finally), *Acarinina pentacamerata* (Subbotina), *Guembeltrioides lozanoi* (Colom),
223 *Planorotalites palmerae* Cushman & Bermudez, *Igorina broedermanni* (Cushman & Bermudez)
224 and *Acarinina pseudotopilensis* Subbotina. This species association is assigned to the late Early
225 Eocene (Late Ypresian).

226

227 **Pp8- *Guembeltrioides nuttalli* - *Globigerinatheka kugleri* Zone (IZ)**

228 Estimated age: 46.4–44.4 Ma (Cande & Kent, 1995); 45.5– 43.4 Ma (Luterbacher *et al.*, 2004);
229 Middle Eocene (Wade *et al.*, 2011).

230 This zone, marked by FO of *Guembeltrioides nuttalli* (Hamilton) and FO of *Globigerinatheka*
231 *kugleri* (Bolli, Loeblich & Tappan 1957), is 14 meters thick (bed Pl 22 to bed Pl 38) (Fig. 5). It
232 corresponds to the Zone P10 (*Hantkenina nuttalli* IZ) of Berggren *et al.* (1995), Zone E8 (*G.*
233 *nuttalli* LOZ) of Berggren & Pearson (2005) and Wade *et al.* (2011). The associated fauna
234 consists of *Dentoglobigerina yeguaensis* (Weinzierl & Applin), *Guembeltrioides lozanoi*
235 (Colom), *Truncorotaloides* sp., *Acarinina bullbrooki* (Bolli), *Turoborotalia frontosa*
236 (Subbotina), *Morozovella caucasica* (Glaessner) and *Morozovella aragonensis* (Nuttall). This
237 zone is assigned to Middle Eocene (Early Lutetian).

238 **Remarks:** the second radiolarian association occurs in the interval from bed Pl 30 to bed Pl 35
239 (Fig. 5).

240

241 **Pp9- *Globigerinatheka kugleri*-*Morozovella aragonensis* Zone (CRZ)**

242 CRZ: Concurrent Range Zone

243 Estimated age: 44.4–43.6 Ma (Cande & Kent, 1995); 43.4– 42.6 Ma (Luterbacher *et al.*, 2004);
244 middle Eocene (Wade *et al.*, 2011).

245 This zone, characterized by the concurrent range of the nominate taxa between the FO of
246 *Globigerinatheka kugleri* (Bolli, Loeblich & Tappan) and the LO (last Occurrence) of
247 *Morozovella aragonensis* (Nuttall), is 8.5 meters thick (bed Pl 38 to bed Pl 45) (Fig. 5). This
248 zone is equivalent to P 11 (*G. kugleri*-*M. aragonensis* CRZ) of Berggren *et al.* (1995) and Zone
249 E 9 (*G. kugleri*-*M. aragonensis* CRZ) of Berggren & Pearson (2005) and Wade *et al.* (2011).
250 This zone also contains *Guembelitrioides nuttalli* (Hamilton), *Acarinina bullbrooki* (Bolli),
251 *Dentoglobigerina yeguaensis* (Weinzierl & Applin), *Globigerinatheka senni* (Beckmann),
252 *Globigerinatheka kugleri* (Bolli, Loeblich & Tappan), *Globigerinatheka index* (Finlay),
253 *Turborotalia possagnoensis* (Toumarkine & Bolli), *Turborotalia frontosa* (Subbotina) and
254 *Morozovella aragonensis* (Nuttall). This association corresponds to the Middle Eocene (Middle
255 Lutetian).

256 **Remarks:** the third radiolarian association occurs in the interval from bed Pl 41 to bed Pl 42
257 (Fig. 5).

258 **Pp10- *Acarinina topilensis* Zone (PRZ)**

259 (PRZ): Partial Range Zone

260 Estimated age: 43.6–42.3 Ma (Cande & Kent, 1995); 42.6–41.4 Ma (Luterbacher *et al.*, 2004);
261 middle Eocene (Wade *et al.*, 2011).

262 This zone defined by the LO of *Morozovella aragonensis* (Nuttall) and the LO of
263 *Guembelitrioides nuttalli* (Hamilton), is 5 meters thick (bed Pl 46 to bed Pl 51) (Fig. 5). It is
264 equivalent to the lower part of P 12 (*M. lehneri*, PRZ) of Berggren *et al.* (1995) and Zone E10
265 (*A. topilensis*, PRZ) of Berggren & Pearson (2005) and of Wade *et al.* (2011). This zone also

266 contains *Acarinina spinuloinflata* (Bandy), *Guembelitrionides nuttalli* (Hamilton),
267 *Globigerinatheka index* (Finlay), *Acarinina topilensis* (Cushman), *Acarinina bullbrooki* (Bolli),
268 *Turboroatlia frontosa* (Subbotina), *Turboroatlia pomeroli* (Toumarkine & Bolli),
269 *Dentoglobigerina yeguaensis* (Weinzierl & Applin), *Morozovella (Morozovelloides) lehneri*
270 (Cushman and Jarvis), *Globigerina praebulloides* Blow, and *Globigerinatheka kugleri* (Bolli,
271 Loeblich & Tappan). Based on planktonic foraminifera, this horizon can be assigned to the
272 Middle Eocene (Middle Lutetian).

273

274 **Pp11- *Morozovelloides lehneri* Partial-Range Zone (PRZ)**

275 Estimated age: 42.3–40.5 Ma (as per Cande & Kent, 1995); 41.4– 39.8 Ma (as per Luterbacher *et*
276 *al.*, 2004); middle Eocene (Lutetian-Bartonian) (Wade *et al.*, 2011).

277 This zone, characterized by the LO of *Guembelitrionides nuttalli* (Hamilton) and LO of *Acarinina*
278 *bullbrooki* (Bolli), is 4 meters thick (bed P1 52 to bed P1 58) (Fig. 5). It is equivalent to the upper
279 part of P12 (*M. lehneri*, PRZ) of Berggren *et al.* (1995) and E11 (*M. lehneri*, PRZ) of Berggren
280 & Pearson (2005) and Wade *et al.* (2011). The associated planktonic fauna contains
281 *Globigerinatheka kugleri* (Bolli, Loeblich and Tappan), *Acarinina topilensis* (Cushman),
282 *Turoborotalia frontosa* (Subbotina), *Dentoglobigerina yeguaensis* (Weinzierl and Applin),
283 *Acarinina bullbrooki* (Bolli), *Globigerinatheka senni* (Beckmann) and *Hantkenina* sp. This
284 association extends through the Late Lutetian-Bartonian age.

285 **Remarks:** The Zone E12 (*Orbulinoides beckmanni* Taxon-range Zone) of Berggren & Pearson
286 (2005) and Wade *et al.* (2011) is absent due to lateral facies change. There, pelagic carbonates of
287 the Pabdeh Fm. corresponding to the planktonic biozone E12, are replaced by an inter-fingered

288 lens of the Jahrum Formation (with benthic foraminifera). This interval has a thickness of 2.5
289 meters (bed Pl 59 to bed Pl 60) (Fig. 5). The benthic foraminifera consist of *Gyrodinella magna*
290 (Le Calvez), *Neorotalia* spp., *Asterigerina rotula* (Kaufmann), and *Discocyclina* sp. and are
291 assigned to the Bartonian.

292

293 **Pp12: *Morozovella crassata*- *Globigerinatheka kugleri* (IZ)**

294 Estimated age: 40.0–38.0 Ma (Cande & Kent, 1995); 39.4– 37.7 Ma (Luterbacher *et al.*, 2004);
295 40.0–38.1 Ma (Pälike *et al.*, 20006) ; Middle Eocene (Bartonian) (Wade *et al.*, 2011).

296 This zone, marked by the FO of *Morozovella crassata* (Cushman) and the LO of
297 *Globigerinatheka kugleri* (Bolli, Loeblich & Tappan), has a thickness of 14 meters (bed Pl 61 to
298 bed Pl 76) (Fig. 5). This zone is equivalent to P14 (*Tr. rohri*-*M. spinulosa* PRZ) of Berggren *et*
299 *al.* (1995), Zone E13 (*M. crassata* HOZ) of Berggren & Pearson (2005) and Zone E13
300 (*Morozovelloides crassatus* HOZ) of Wade *et al.* (2011). The biostratigraphic range is assigned
301 to the Bartonian.

302 The planktonic fauna is as follows: *Globigerinatheka kugleri* (Bolli, Loeblich & Tappan),
303 *Morozovella crassata* (Cushman), *Catapsydrax dissimilis* Cushman & Bermudez,
304 *Dentoglobigerina yeguaensis* (Weinzierl & Applin), *Subbotina eocaenica* (Guembel),
305 *Turborotalia pomeroli* Toumarkine & Bolli, *Turborotalia griffinae* Blow, *Pseudohastigerina*
306 *micra* (Cole), *Turborotalia increbescens* Bandy, *Globigerinatheka index* (Finlay),
307 *Globigerinatheka Mexicana* (Cushman), *Globigerinatheka luterbacheri* Bolli, *Turborotalia*
308 *cerroazulensis* (Cole), *Pseudohastigerina* sp. and *Hantkenina* sp.

309 In this interval (from bed Pl 61 to bed Pl 76), two inter-fingered lenses of Jahrum Formation
310 containing benthic foraminifera are observed. The first lens contains *Gyrodinella magna* (Le
311 Calvez), *Asterigerina rotula* (Kaufmann), *Gypsina marianensis* Hanzawa, *Nummulites fossulata*
312 De Cizancourt, and *Discocyclina* sp. It has a thickness of 3.5 meters and extends from bed Pl 64
313 to bed 68 (Fig. 6). The second horizon contains *Neorotalia* spp., *Discocyclina* sp., *Gyroidinella*
314 *magna* (Le Calvez), *Gypsina marianensis* Hanzawa, and *Asterocyclina sireli* Özcan & Less. It
315 presents a thickness of 3.5 meters and extends from bed Pl 72 to Pl 74 (Fig. 6). Based on benthic
316 foraminiferal association, the biostratigraphic range of both lenses is considered Bartonian.

317

318 **Pp13- *Cribrohantkenina inflata*- *Globigerinatheka Mexicana* Zone (IZ)**

319 Estimated age: 38.0–35.8 Ma (Cande & Kent, 1995); 37.7– 35.8 Ma (Luterbacher *et al.*, 2004);
320 38.1–35.8 Ma (Pälike *et al.*, 2006); Middle-Late Eocene (Bartonian-Priabonian) (Wade *et al.*,
321 2011).

322 This zone, characterized by FO of *Cribrohantkenina inflata* Howe to LO of *Globigerinatheka*
323 *Mexicana* (Cushman) is 4.5 meters thick (bed Pl 75 to bed Pl 83) (Fig. 5). It is equivalent to
324 Zone P15 (*Po. semiinvoluta* IZ) of Berggren *et al.* (1995) and Zone E14 (*G. semiinvoluta* HOZ)
325 of Berggren & Pearson (2005) and Wade *et al.* (2011). The associated planktonic fauna contains
326 *Turborotalia cerroazulensis* (Cole), *Turborotalia pomeroli* (Toumarkine & Bolli), *Catapsydrax*
327 *dissimilis* Cushman & Bermudez, *Globigerinatheka index* (Finlay), *Turborotalia increbescens*
328 Bandy, *Globigerina venezuelana* (Hedberg), and *Cribrohantkenina inflata* Howe.

329

330 **Pp14: *Globigerinatheka index* Zone (PRZ)**

331 **PRZ: Partial Range Zone**

332 This zone, characterized by the partial range of the nominate taxa between the LO of
333 *Globigerinatheka Mexicana* (Cushman) and the LO of *Globigerinatheka lutherbacheri* Bolli,
334 extends over a thickness of 10 meters (bed Pl 83 to bed Pl 99) (Fig. 5). The associated
335 planktonic fauna is *Pseudohastigerina nagewichiensis* (Myatliuk), *Cribrohantkenina inflata*
336 Howe, *Turborotalia cocoaensis* (Cushman), *Turborotalia cerroazulensis* (Cole), *Globigerina*
337 (*Dentoglobigerina*) *venezuelana* (Hedberg), *Pseudohastigerina micra* (Cole), *Turborotalia*
338 *pomeroli* (Toumarkine and Bolli), *Catapsydrax dissimilis* Cushman and Bermudez, *Turborotalia*
339 *increbescens* Bandy, *Globigerinatheka Mexicana* (Cushman) and *Globigerinatheka*
340 *lutherbacheri* Bolli.

341 Two horizons with benthic foraminifera are observed in this biozone. They can be correlated
342 with the zone E15 of Berggren & Pearson (2005) and Wade *et al.* (2011). The first horizon 4.5
343 meters thick, extends from bed Pl 85 to bed 90 (Fig. 6). It consists of *Fabiania cubensis*
344 (Cushman & Bermudez), *Chapmanina gassinensis* (Silvestri), *Penarchaias cf. glynnjonesi*
345 (Henson), *Praebullalveolina afyonica* Sirel & Acar, *Halkyardia* sp., *Silvestriella cf. tetraedra*
346 Gumbel, *Discocyclina nandori* Less, *Nummulites cf. fabianii* (Prever), *Borelis* sp., *Gyroidinella*
347 *magna* (Le Calvez), *Neortalia* spp., *Praerhapydionina* sp., and *Discocyclina* sp. The second
348 horizon presents a thickness of 1.5 meters and extends from bed 94 to bed 97. It contains
349 *Chapmanina gassinensis* (Silvestri), *Nummulites cf. fabianii* (Prever), and *Neorotalia* spp. (Fig.
350 6). This association is equivalent to E15 of Berggren & Pearson (2005) and Wade *et al.* (2011)
351 and can be assigned to the Priabonian due to the presence of *Nummulites cf. fabianii* (Prever).

352 The rest of the columnar section (top of section) with a thickness of 22.5 meters (bed 100 to bed
353 111) is formed by the Jahrum Formation. It contains *Alveolina nuttalli* (Davies), *Discocyclusina*
354 *nandori* Less, *Asterigerina rotula* (Kaufmann), *Macetadiscus incolumnatus* Hottinger, and
355 *Discocyclusina* sp. This benthic foraminiferal association is equivalent to E16 of Berggren &
356 Pearson (2005) and Wade et al. (2011). The range of this association is assigned to the
357 Priabonian.

358

359 4. PALEOENVIRONMENT REMARKS

360 The lithologic units may change laterally from a continuous to abrupt fashion (Boggs (2006).
361 Facies changes may occur as lateral gradation, pinch out, or inter-tonguing/inter-fingering. The
362 abrupt contacts (inter-tonguing), which are commonly very sharp can distinctly separate two
363 formations with different lithologies a result of fast changes in local depositional conditions. The
364 pelagic and hemipelagic facies of the Pabdeh Formation are deposited in deep-sea (open ocean)
365 environment. They consist of argillaceous limestones, mudstones, and radiolarian cherts. The
366 argillaceous limestones mostly contain planktonic foraminifera such as *Acarinia*, *Morozovella*,
367 *Globigerinatheka*, *Turborotalia*, etc. The stratigraphical analysis of the Pabdeh Formation
368 showed the presence of some inter-fingering layers of the Jahrum Formation containing benthic
369 foraminifera only, which correspond to shallow marine neritic deposits. The occurrence of inter-
370 fingered tongues of benthic facies (Jahrum Formation) within the pelagic facies (Pabdeh
371 Formation) suggests repeated sharp depth changes (Fig. 3B). In addition, the appearance of
372 medium to coarse grain bioclastic limestone with larger benthic foraminifera and large-sized red
373 algae in the top of the section (Jahrum Fm.) suggests shallowing. Hence, the overlapping benthic
374 facies on top of the section recorded regression that could be due to progressive shrinking of the

375 basin and sea-level drop as well. The gradual decline of micrite observed in the Jahrum
376 Formation is likely due to decreasing water depth and increasing energy, which led to the
377 development of bioclastic limestone. Concomitantly, the benthic foraminifers are mainly limited
378 to rotaliids (*Gyroidinella*, *Fabiania*, etc.), orthophragminids (*Discoyclina*), and alveolinids,
379 which indicate restricted platform conditions (Murray 1991; Hottinger 1983, 1997; Flugel 1982,
380 2004).

381

382 5. DISCUSSION

383 The studied section mainly consists of Pabdeh Formation with some inter-fingered tongues of
384 Jahrum Formation. Based on lithological features, the Pabdeh Formation is subdivided into two
385 lithological units (Lower and Upper Units). The Lower Unit is dominated by pelagic limestone
386 and radiolarian chert, whereas the Upper Unit consists of pelagic limestone, mudstone, and some
387 inter-fingered lenses of bioclastic limestone, which are attributed to the Jahrum Formation.
388 Further up, toward the top of the section, the Pabdeh formation is overlain by the Jahrum
389 Formation represented by a carbonate succession of packstone with abundant red algae,
390 bioclasts, and hyaline/porcellaneous foraminifers.

391 The presence of marker planktonic foraminifera such as *Acarinina subsphaerica* (Subbotina)
392 confirms the Late Paleocene age of Zone Pp1, because the last occurrence of this species falls in
393 the upper part of Zone Pp1. The species *Morozovella velascoensis* (Cushman) occurs across the
394 Late Paleocene-Early Eocene boundary, therefore its presence help to distinguish the Zone Pp2.
395 During the Early Eocene from the upper part of Zone Pp2 to Zone Pp7, some taxa such as

396 *Morozovella* and *Turborotalia* were rare but *Igorina broedermanni* (Cushman and Bermudez)
397 was only sporadic during the Early Eocene (Ypresian).

398 The Lutetian stage (from Zone Pp8 to Zone Pp10) coincides with the extinction of some species
399 such as *Planorotalites palmerae* Cushman and Bermudez, *Acarinina pseudotopilensis* Subbotina,
400 *Turborotalia prolata* (Belfoed), and *Acarinina pentacamerata* (Subbotina). In contrast, the
401 association of *Acarinina bullbrooki* (Bolli), *Globigerinatheka kugleri* (Bolli, Loeblich &
402 Tappan), *Turborotalia possagnoensis* (Toumarkine & Bolli), *Acarinina topilensis* (Cushman),
403 *Dentoglobigerina yeguaensis* (Weinzierl & Applin), *Globigerinatheka senni* (Beckmann),
404 *Guembelitrioides nuttalli* (Hamilton), *Turborotalia frontosa* (Subbotina), *Turborotalia*
405 *possagnoensis* (Toumarkine & Bolli), and *Morozovella aragonensis* (Nuttall) are abundant.

406 The time interval Lutetian-Bartonian is equivalent to Zone Pp11, which is consistent with Zone
407 E11 of Berggren & Pearson (2005). It is characterized by the partial range zone of *Morozovella*
408 *lehneri* (Cushman & Jarvis).

409 Abundant Bartonian planktonic foraminifers are represented in the Zone Pp12 of this study, but
410 some species such as *Turborotalia griffinae* Blow, *Pseudohastigerina micra* (Cole),
411 *Globigerinatheka Mexicana* (Cushman), *Globigerinatheka lutherbacheri* Bolli, *Turborotalia*
412 *increbescens* Bandy, *Turborotalia cerroazulensis* (Cole), *Pseudohastigerina* sp. and *Hantkenina*
413 sp. are rare in this biozone. In contrast, they are abundant in the Zone Pp13 for the Bartonian-
414 Priabonian time interval. The species *Globigerinatheka kugleri* (Bolli, Loeblich & Tappan)
415 becomes extinct in this biozone, whereas the species *Globigerina* (*Dentoglobigerina*)
416 *venezuelana* (Hedberg), and *Cribohantkenina inflata* Howe are reported for the first time.

417 Three associations of benthic foraminifera (Fig. 6) are distinguished in the middle and upper
418 parts of the stratigraphic section. They are assigned to the Bartonian and Priabonian stages and
419 can be equivalent with Zone Pp 12 –Zone Pp14.

420

421 5. CONCLUSION

422 - The Pabdeh Formation is mainly composed of hemipelagic and pelagic sediments with
423 intercalations of radiolarian chert, whereas the Jahrum Formation consists of neritic deposits
424 accumulated on a shallow marine platform. Both formations are disconformably covered by the
425 Late Oligocene-Miocene Asmari Formation.

426 -The Pabdeh Formation consists of Late-Paleocene to Late Eocene planktonic foraminifera
427 (Zone Pp1–Pp14) which correlate mainly to the subtropical to tropical Zones P4b-E15 of
428 Berggren & Pearson (2005). This Formation passes upwards and laterally into the Jahrum
429 Formation and up section. Hence, the abrupt disappearance of the planktonic foraminifera in the
430 Pabdeh Formation coincides with the presence of larger benthic foraminifera (orthophragminids,
431 rotaliids) in the Jahrum Formation.

432 -The orthophragminids (*Discocyclina*) are mainly associated with rotaliids (*Gyroidinella*,
433 *Asterigerina*, etc), while alveolinids and nummulitids are locally relatively common in the
434 bioclastic facies of Jahrum Formation. The low frequency of *Nummulites* and major changes in
435 the composition of benthic foraminifera with increasing rotalides recorded a change of
436 sedimentary environment.

437 -The occurrence of Jahrum Formation (bearing benthic foraminifera) within the Pabdeh
438 Formation (bearing planktonic foraminifera) enables benthic foraminifera ranges to be tied to

439 local planktonic foraminiferal biostratigraphy. Therefore, the stratigraphic range of benthic
440 foraminiferal associations in the upper part of the study section is Bartonian-Priabonian.

441 -Late Paleocene planktonic foraminifera are sparse in the Pabdeh Formation, whereas the Eocene
442 planktonic foraminifers are more abundant and widespread.

443 -During the Early Eocene, the two genera *Acarinina* and *Morozovella* are abundant but other
444 genera such as *Globigerinatheca*, *Turborotalia*, etc. gradually become predominant.

445 -The absence of open marine planktonic foraminifera such as *Orbulinoides beckmanni*, which
446 corresponds to Zone E12 of Berggren and Pearson (2005) in the upper unit of Pabdeh Formation,
447 coincides with the sudden appearance of larger benthic foraminifera coeval with coarsening
448 upwards trend. As this interval coincides with the Middle Eocene Climate Optimum (ca. 40 Ma),
449 which corresponds to a sea level rise of ca. 50 m (e.g. Miller et al., 2020 and references therein),
450 such abrupt shallowing recorded by the absence of planktonic foraminifers must be due to
451 tectonic causes.

452 **ACKNOWLEDGEMENTS**

453 we thank Borzou Asgari Pirbaloti and Zahra Shaiesteh Nia for their generous help during
454 fieldwork. The first author is grateful to the Payame Noor University of Iran for the support of
455 this scientific project.

456

457 **REFERENCES**

458 Adams T. D. & Bourgeois F. 1967. Asmari biostratigraphy, Geological and Exploration
459 Division. *Iranian Oil Offshore Company Report*, 1074 (Unpublished).

460 Ahmad S., Jalal W., Ali F., Hanif M., Ullah Z., Khan S., Ali A., Jan UI. & Rehman K. 2014.
461 Using larger benthic foraminifera for the paleogeographic reconstruction of Neo-Tethys during
462 Paleogene. *Arabian Journal Geoscience*, 1-18.

463 Alavi M. 2004. Regional Stratigraphy of Zagros Fold-Thrust Belt of Iran and Its Proforel and
464 Evolution. *American Journal of Science*, 304: 1-20.

465 Babazadeh S. A. 2003. Biostratigraphie et contrôles paléogéographiques de la zone de suture de
466 l'Iran oriental. Implications sur la fermeture Téthysienne. Thèse de doctorat, Université
467 d'Orléans, France 1-384.

468 Babazadeh S. A., Baharan S., Parvaneh Nezhad Shirazi & Bahrami M. 2010. Biostratigraphy of
469 Pabdeh Formation in Tange Zahjiran section (southeast Shiraz) based on planktic foraminifera.
470 *Sedimentology and stratigraphy Reserches*, 38(1): 145-158.

471 Babazadeh S. A., Moghadasi S. J. & Yoosefizadeh Baghestani N. 2015. Analysis of sedimentary
472 basin based on the distribution of microfacies of Jahrom Formation in Dashte Zari, Shahrekord.
473 *18th geology conference of Iran, Tarbiat Modares University*, 649-655.

474 Berberian M., 1995, Master "blind" thrust faults hidden under the Zagros folds: active basement
475 tectonics and surface morphotectonics: *Tectonophysics*, 241(3-4), 193-224.

476 Berberian M. & King G. C. P. 1981. Towards a Paleogeography and Tectonic Evolution of Iran.
477 *Canadian Journal of Earth Sciences*, 18: 210-265.

478 Berggren W. A., Kent D. V., Swisher I. C. C. & Aubry M. P. 1995. A revised Cenozoic
479 geochronology and chronostratigraphy. *In: Berggren W.A., Kent D.V., Aubry M. P. &*
480 *Hardenbol J. (Eds). Geochronology, Time Scales and Global Stratigraphic Correlations: Society*
481 *of Economic Paleontologists and Mineralogists Special Publication*, 54:129-212.

482 Berggren W. A. & Pearson P. 2005. A Revised Tropical to Subtropical Paleogene Planktonic
483 Foraminiferal Zonation. *The Journal of Foraminiferal Research*, 35: 279- 298.

484 Berggren W. A, Pearson P. N., Huber B. T. & Wade B.S., 2006. Taxonomy, biostratigraphy, and
485 phylogeny of Eocene *Acarinina*. *Cushman Foundation special publication*, 41: 257-326.

486 Boggs, S. 2006, *Principles of Sedimentology and Stratigraphy* (third ed.), Pearson Education,
487 p. 676.

488 Cande S. C. & Kent D. V. 1995. Revised calibration of the geomagnetic polarity timescale for
489 the Late Cretaceous and Cenozoic. *J. Geophys. Res.*, 100: 6093–6095.

490 Chegni F., Baghbani D., Vaziri S. H. Mohtat T. & Ghadimvand Kohansal N. 2016.
491 Biostratigraphy of Pabdeh Fm. (Middle-Late Eocene) in south Kuh-e-Mishan and Kuh-e-Eshgar
492 in Izeh, west Kazeron fault. *Earth sciences, Geological Survey of Iran*, 99: 143-156.

493 Cole W. S. & Gravell D. W. 1952. Middle Eocene Foraminifera from Peñon Seep, Matanzas
494 Province, Cuba. *Journal of Paleontology*. 26(5): 708-727.

495 Daneshian J., Shariati S. and Salsani A. 2015. Biostratigraphy and planktonic foraminiferal
496 abundance in the phosphate-bearing Pabdeh Formation of the Lar Mountains (SW Iran). *N. Jb.*
497 *Geol. Paläont. Abh., Stuttgart*, 1-16.

498 Davoudzadeh M. & Schmidt K., 1981. Contribution to the paleogeography and stratigraphy of
499 the Upper Triassic to Middle Jurassic of Iran. *Neues Jahrbuch für Geologie und Paläontologie,*
500 *Abhandlungen* 162, 137–163.

501 Ehrenberg S. N., Pickard N. A.H., Laursen G.V., Monibi S., Mossadegh Z. K.,T. Svånå A.,
502 Aqrawi A. A.M., McArthur J. M. and Thirlwall M. F. (2007). Strontium isotope stratigraphy of
503 the Asmari Formation (Oligocene - Lower Miocene), SW Iran. *Journal of Petroleum Geology*,
504 30(2), 107-128.

505 Ellis B. F. & Messina A. 1940. *Catalogue of Foraminifera*. Micropaleontology Press, American
506 *Museum of Natural History, New York.*

507 Flugel E. 1982. *Microfacies analysis of limestones*. Berlin, Springer-Verlag, 633 p.

508 Flugel E. 2004. *Microfacies of carbonate rock*, Springer-Verlag, 976 p.

509 Hadavandkhani N., Sadeghi A., Adabi M. H. & Tahmasbi A. R. 2018. Lithostratigraphy and
510 biostratigraphy of Pabdeh Formation in Chaharda village section (Izeh, Khuzestan). *Earth*
511 *sciences, Geological Survey of Iran*, 107: 137-150.

512 Hanzawa S. 1957. Cenozoic Foraminifera of Micronesia. *Geological Society of America*. 66: 163
513 p.

514 Hayward B. W., Le Coze F., Vachard D. & Gross O. 2021. World Foraminifera Database,
515 *Fabiania cubensis*. <https://marinespecies.org/foraminifera/aphia>.

516 Hottinger L. 1983. Processes determining the distribution of larger foraminifera in space and
517 time. *Utrecht Micropaleont Bull.*, 30: 239–253.

518 Hottinger L. 1997. Shallow benthic foraminiferal assemblages as signals for depth of their
519 deposition and their limitations. *Bulletin de la Société Géologique de France*, 168 (4): 491-505.

520 Hottinger L. 2007. Revision of the foraminiferal genus *Globoreticulina* Rahaghi, 1978, and of its
521 associated fauna of larger foraminifera from the late Middle Eocene of Iran. *Carnets de Géologie*
522 */Notebooks on Geology*, 51 p.

523 James G. A. & Wynd J. G. 1965. Stratigraphic Nomenclature of Iranian Oil Consortium
524 Agreement Area. *American Association of Petroleum Geologists Bulletin*, 49: 94-156.

525 Kalantari A. 1976. Microbiostratigraphy of the Sarvestan Area, Southwestern Iran (Geological
526 Laboratories Publication). *National Iranian Oil Company*, 1-129.

- 527 Kalantari A. 1978. Paleocene Biostratigraphy of some parts of Iran (Geological Laboratories
528 Publication). *National Iranian Oil Company*, 1-165.
- 529 Kalantari A. 1980. Tertiary Faunal Assemblage of Qum-Kashan, Sabzevar and Jahrum areas
530 (Geological Laboratories Publication), *National Iranian Oil Company*, 1-126.
- 531 Kalantari A. 1986. Microfacies of Carbonate Rocks of Iran. *National Iranian Oil Company*,
532 *Geological Laboratories*, 1-520.
- 533 Khatibi Mehr M. & Moalemi A. 2009. Historical sedimentary correlation between Jahrom
534 Formation and Ziarat Formation on the basis of benthic foraminifera. *Journal of Geology of Iran*,
535 9: 87-102.
- 536 Konijnenburg J. H. V., Wernli R. & Bernoulli D. 1998. Tentative biostratigraphy of Paleogene
537 planktic foraminifera in thin-section, an example from the Gran Sasso d'Italia (central
538 Apennines, Italy). *Eclogae Geologicae Helvetiae*, 203-216.
- 539 Le Calvez Y. 1949. Révision des foraminifères lutétiens du Bassin de Paris II, Rotaliidae et
540 familles affines. *Mémoires pour servir à l'explication de la carte géologique détaillée de la*
541 *France*, 1-41.
- 542 Loeblich A. R. & Tappan H. 1987. *Foraminiferal genera and their classification*. Van Nostrand
543 Reinhold Co., New York, 970 p.
- 544 Luterbacher H. P., Ali J. R., Brinkhuis H., Gradstein F. M., Hooker J., Monechi, S., Ogg J. G.,
545 Powell J., Röhl U., Sanphilippo A. & Schmitz B. 2004. The Paleogene Period. *In*: Gradstein F.,
546 Ogg J. & Smith A. (Eds.). *A Geologic Time Scale*. *Cambridge University Press*, 384–408.

547 Miller K.G., Browning J.V., Schmelz W.J., Kopp R.K., Mountain G.S., & Wright J.D. 2020.
548 Cenozoic sea-level and cryospheric evolution from deep-sea geochemical and continental margin
549 records. *Science Advances* 2020; 6 : eaaz1346

550 Moradian F. & Baghbani D. 2016. Lithostratigraphy, biostratigraphy of Paleocene-lower Eocene
551 sequences in Dezful embayment, southwest Iran. *Iranian Journal of Earth Sciences*, 8: 135-146.

552 Moradian F., Baghbani D. & Allameh M. 2017. Microbiostratigraphy of the Paleocene-Lower
553 Eocene Sequences in the Bibi Hakimeh 2 Subsurface Section Located in the SW of Iran. *Open*
554 *Journal of Geology*, 7: 147-161

555 Motiei H. 1994. Geology of Iran: Stratigraphy of Zagros. *Geological Survey of Iran Publication*,
556 583pp.

557 Murray J.W. 1991. Ecology and Palaeoecology of Benthic Foraminifera. *Longman Science &*
558 *Technology*, 397 p.

559 Olsson R. K., Hemleben C., Berggren W. A. & Huber B. T. 1999. Atlas of Paleocene Planktonic
560 Foraminifera. Smithsonian Institution Press, Washington DC, 252 p.

561 Ozgen N. 2000. *Nurdanella boluensis* n.gen., n.sp., a Miliolid (Foraminifera) from the Lutetian
562 of the Bolu Area (Northwestern Turkey). *Revue de paleobiologie*, 19: 79-85.

563 Pälike H., Norris R. D., Herrle J. O., Wilson P. A., Coxall H. K., Lear C. H., Shackleton N. J.,
564 Tripathi A. K., Wade B. S., 2006. The heartbeat of the Oligocene climate system. *Science* 314:
565 1894–1898.

566 Postuma S. A. 1971. Manual of Planktonic Foraminifera: Elsevier, Amsterdam, 420 p.

567 Premoli Silva I. & Bolli H. M. 1973. Late Cretaceous to Eocene planktonic foraminifera and
568 stratigraphy of leg 15, Sites in the Caribbean Sea: *Initial Reports DSDP*, 15: 449–547.

569 Premoli Silva I., Rettori R. & Verga D. 2003. Practical Manual of Paleocene and Eocene
570 Planktonic Foraminifera: *International School on planktonic foraminifera*, second course,
571 Perugia.

572 Rahaghi A. 1976. Contribution à l'étude de quelques grands foraminifères de l'Iran. *National*
573 *Iranian Oil Company*, 6: 1-84.

574 Rahaghi A. 1978. Paleogene biostratigraphy of some parts of Iran. *National Iranian Oil*
575 *Company*, 7:1-165.

576 Rahaghi A. 1980. Tertiary faunal assemblage of Qom-Kashan, Sabzewar and Jahrom area.
577 *National Iranian Oil Company*, 8: 1-126.

578 Rahaghi A. 1983. Stratigraphy and faunal assemblage of Paleocene and Lower Eocene in Iran.
579 *National Iranian Oil Company*, 10: 1-173.

580 Sari B. 2017. Lithostratigraphy and planktonic foraminifera of the uppermost Cretaceous–Upper
581 Palaeocene strata of the Tavas nappe of the Lycian nappes (SW Turkey). *Geologia Croatica*, 70
582 (3): 163-177.

583 Sarigul V., Hakyemez A., Tuysuz, O., Can Genc S., Yilmaz I. O. & Ozcan E. 2017.
584 Maastrichtian-Thonetian planktonic foraminiferal biostratigraphy and remarks on the K-Pg
585 boundary in the southern Kocaeli Peninsula (NW Turkey). *Turkish Journal of Earth Sciences*,
586 26: 1-29.

587 Sengör A. M., Altiner C. Cin D., Ustomer T. & Hsu K. J. 1988. The origin and assembly of the
588 Tethyside orogenic collage at the expense of Gondwana land : *In* : Audley-Charles, M. G. & A.
589 Hallam (eds), Gondwana and Tethys. *Geological Society, Special Publication*, 37 : 119-181.
590

591 Serra-Kiel J. S., Hottinger L., Caus E., Drobne K., Ferrandez C., Jauhir A. K., Less G.,
592 Pavlovec R., Pignatti J., Samso J. M., Schaub H., Sirel E., Strougot A., Tambareau Y.,
593 Toosquella J. & Zakrevskaya E. 1998. Larger foraminiferal biostratigraphy of the Tethyan
594 Palaeocene and Eocene. *Bulletin de la Societe Géologique de France*, 169: 281-299.

595 Sirel E. 2003. Foraminiferal description and biostratigraphy of the Bartonian, Priabonian, and
596 Oligocene shallow-water sediments of southern and eastern Turkey. *Revue de Paléobiologie*, 22:
597 269–339.

598 Sirel E. 2009. Reference sections and key localities of the Paleocene stages and their very
599 shallow/shallow-water three new benthic foraminifera in Turkey. *Revue de Paléobiologie*, 28(2):
600 413-435.

601 Stöcklin J. 1968. Structural History and Tectonics of Iran: A Review. *AAPG Bulletin* (1968) 52
602 (7): 1229–1258.

603 Stöcklin, J. 1977. Structural Correlation of the Alpine Ranges between Iran and Central Asia.
604 *Mémoires de la Société Géologique de France*, 8, 333-353.

605 Stöcklin J. & Setudehnia A. 1991. *Stratigraphic Lexicon of Iran*, Geological Survey of Iran, 18:
606 376pp.

607 Stoneley R., 1981, The geology of the Kuh-e Dalneshin area of Southern Iran, and its bearing on
608 the evolution of Southern Tethys: *Journal of the Geological Society*, London, 138, 509–526.

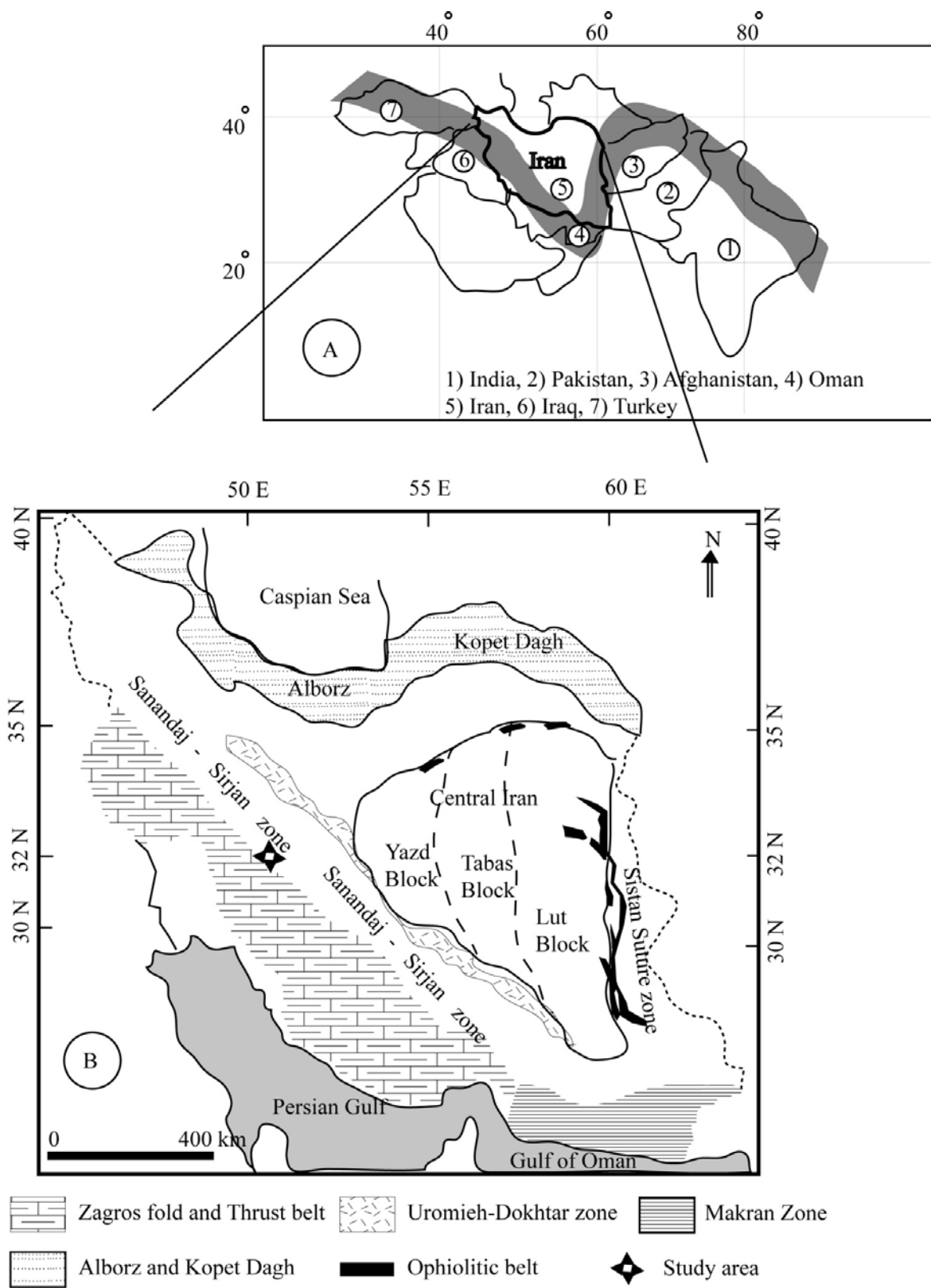
609 Toumarkine M. & Luterbacher H. P. 1985. Paleocene and Eocene Planktic Foraminifera *In*:
610 Bolli H. M., Saunders J. B. & Perch-Nielsen K. (Eds). *Plankton Stratigraphy*: Cambridge
611 University Press, Cambridge, 87-154

612 Wade B. S., Pearson P. N., Berggren W. A. & Palike H. 2011. Review and revision of Cenozoic
613 tropical planktonic foraminiferal biostratigraphy and calibration to the geomagnetic polarity and
614 astronomical time scale. *Earth Science Review*, 104: 111-142.

615 Wernli R., Morend D & Piguet B. 1997. Les foraminifères planctoniques en sections de l'Eocène
616 et de l'Oligocène des Grès de Samoëns (Ultra-helvétique du massif de Platé. Haute-Savoie.
617 France). *Eclogae geol. Helv.*, 90: 581-590.

618 Zahedi M. & Rahmati Ilkhechi M. 2006. Explanation of Geology of Shahrekord quadrangle, 1:
619 250000, 194p.

620



621 Fig. 1

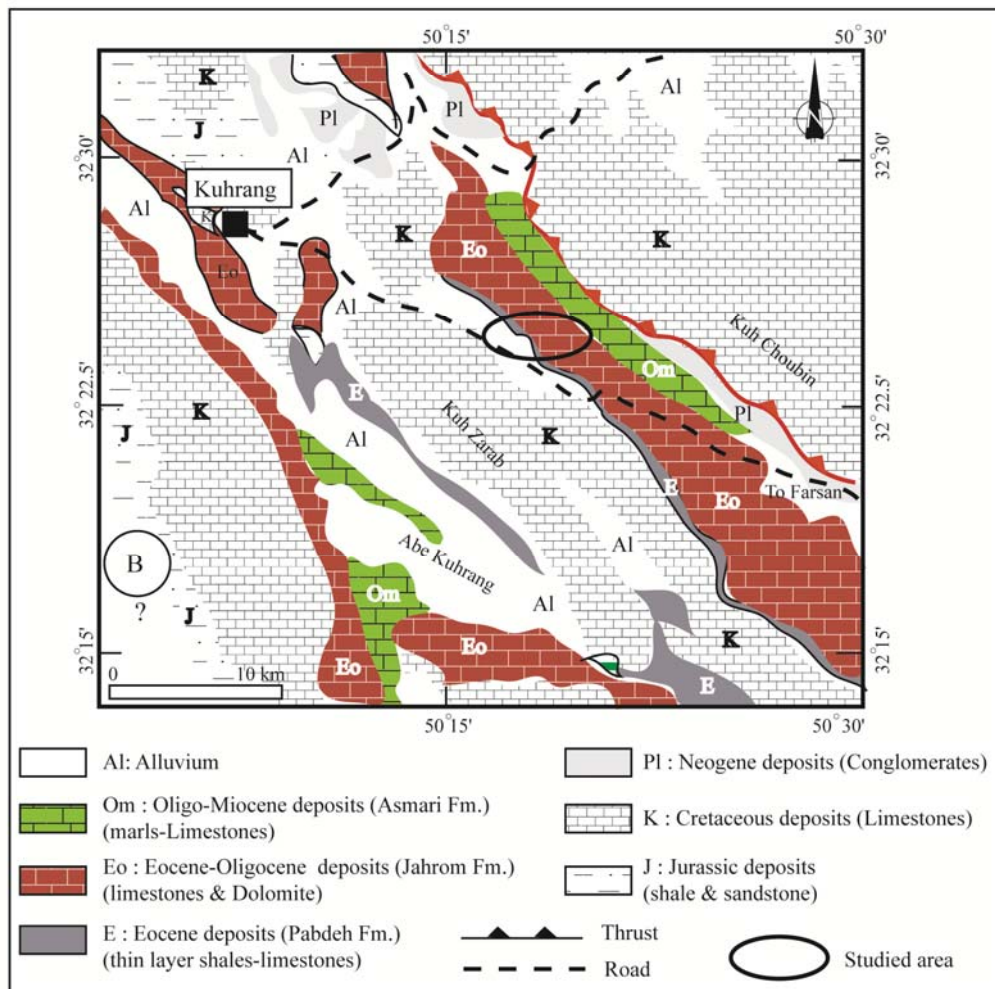
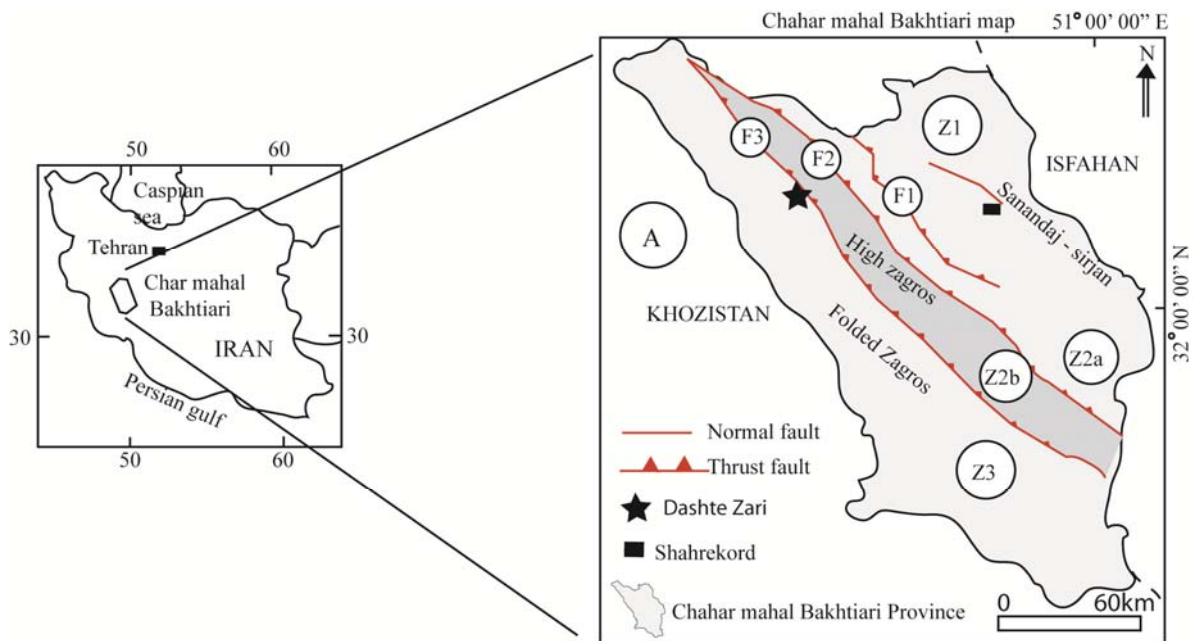


Fig. 2

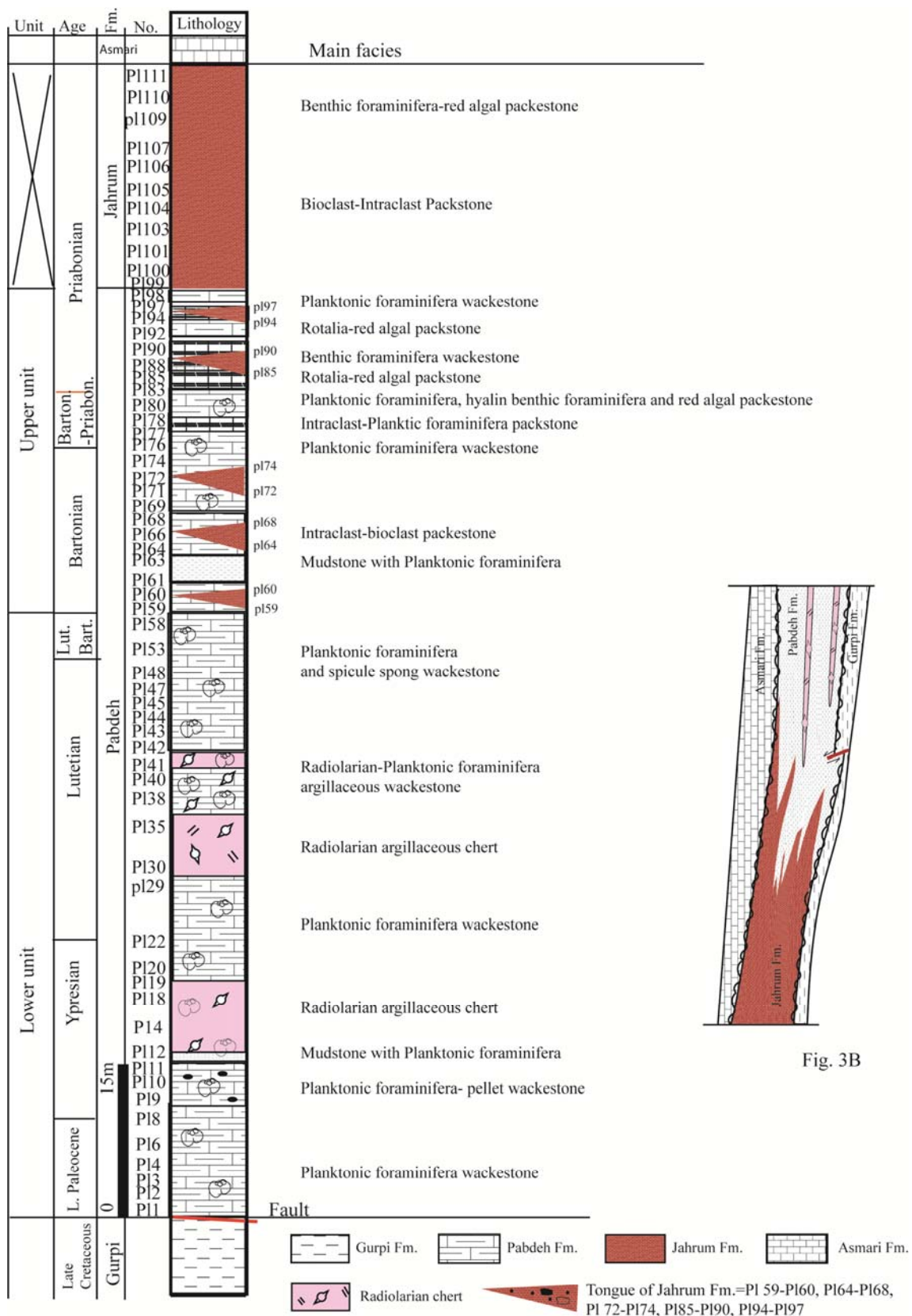


Fig. 3A

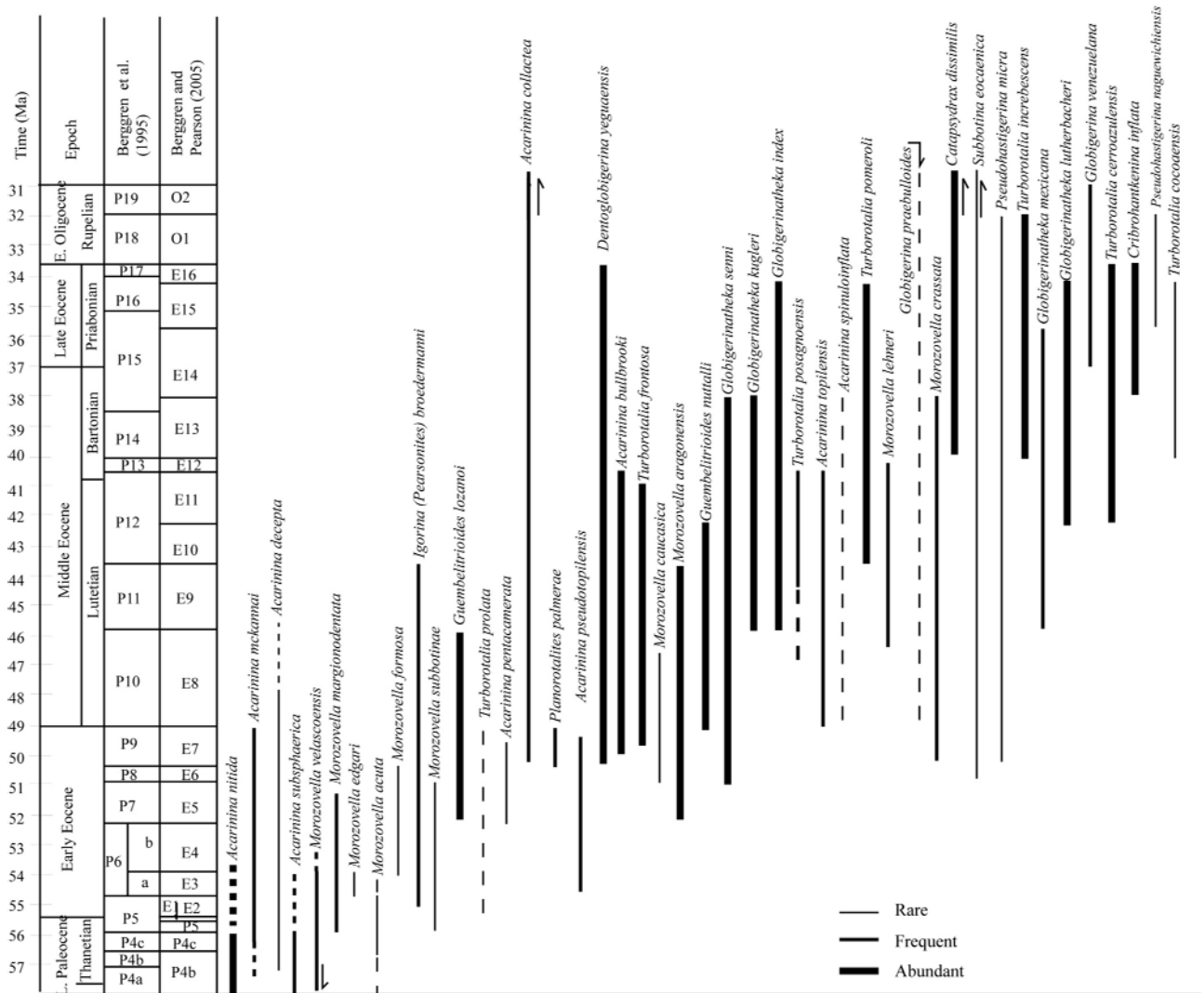


Fig. 4 A

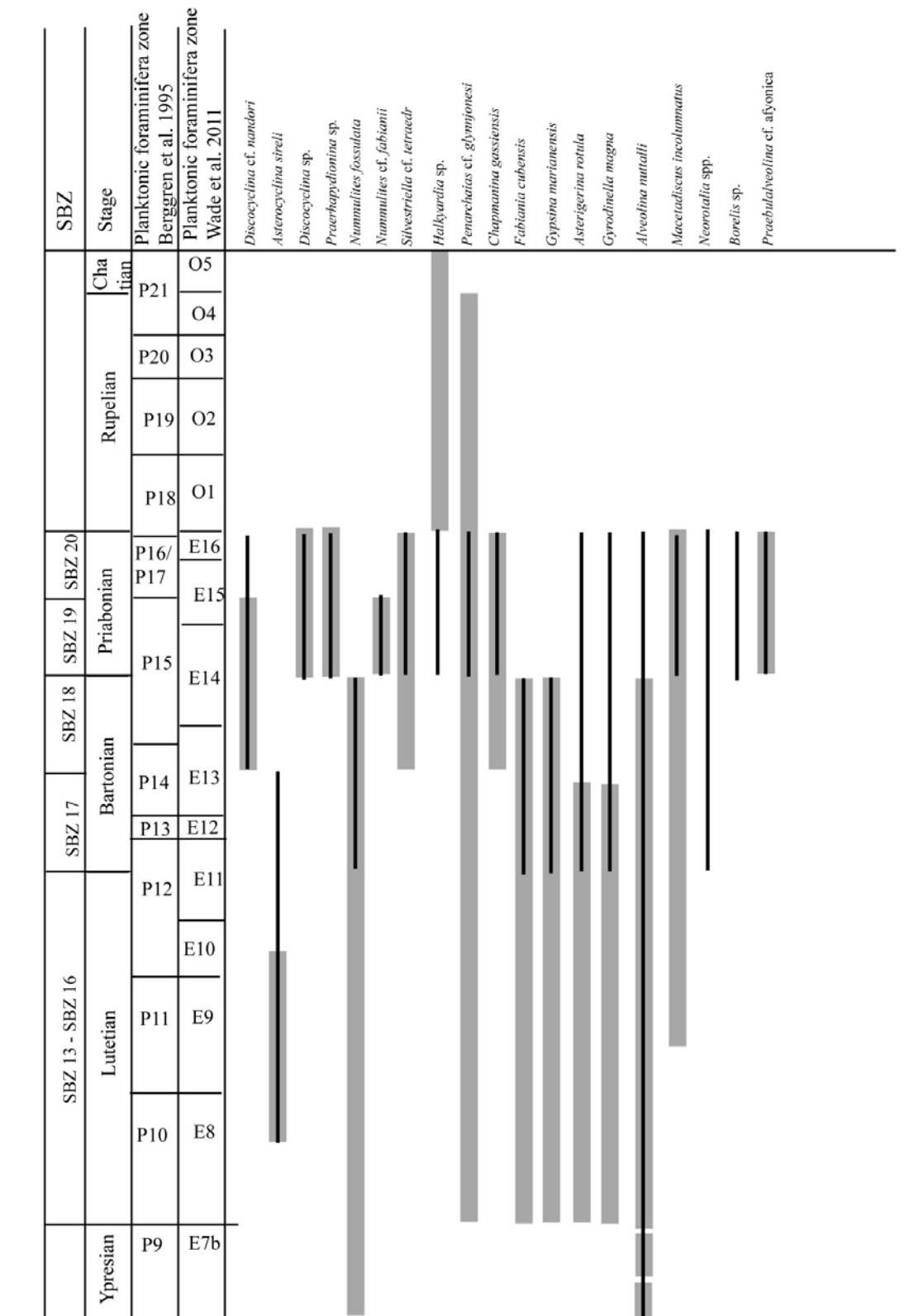
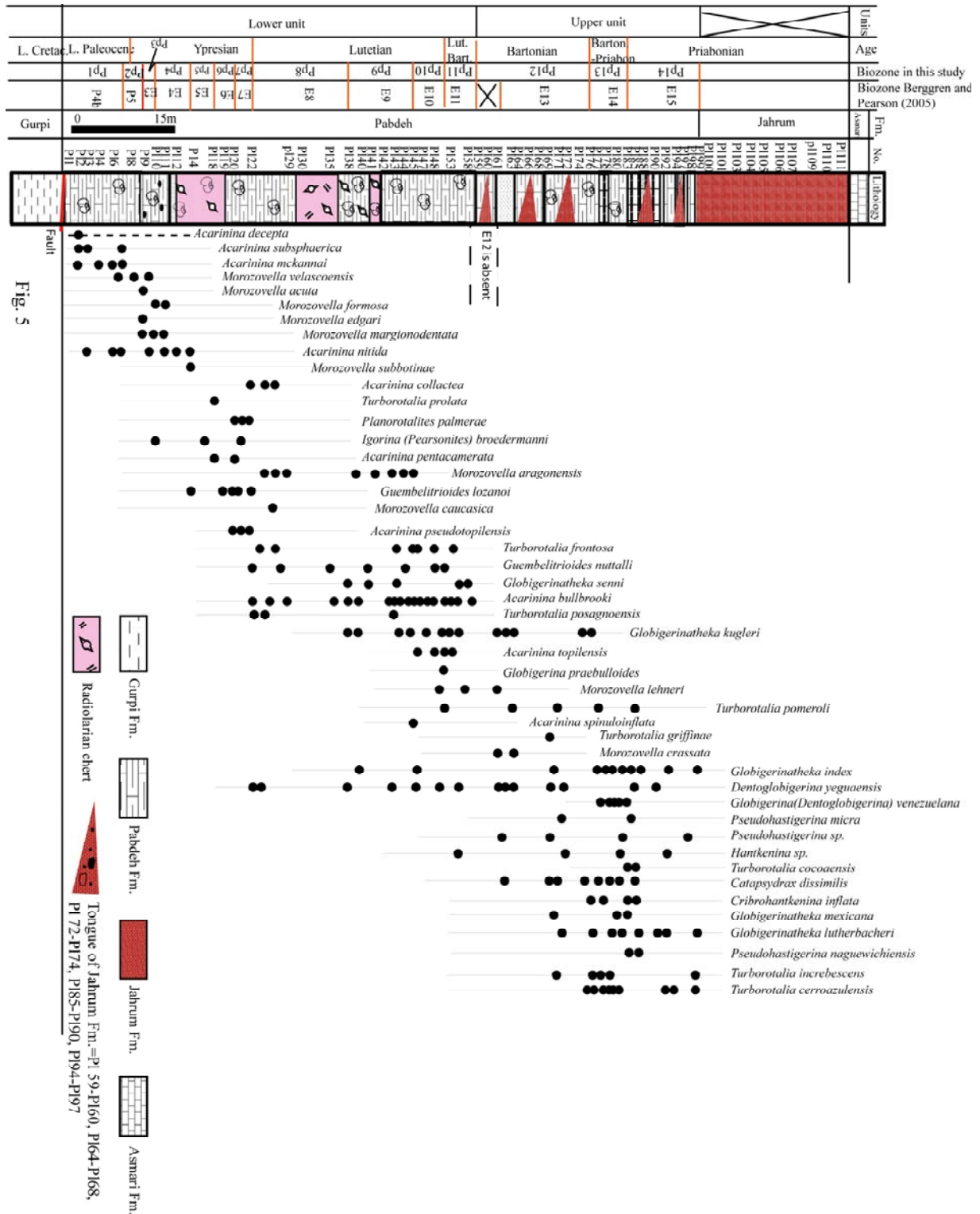
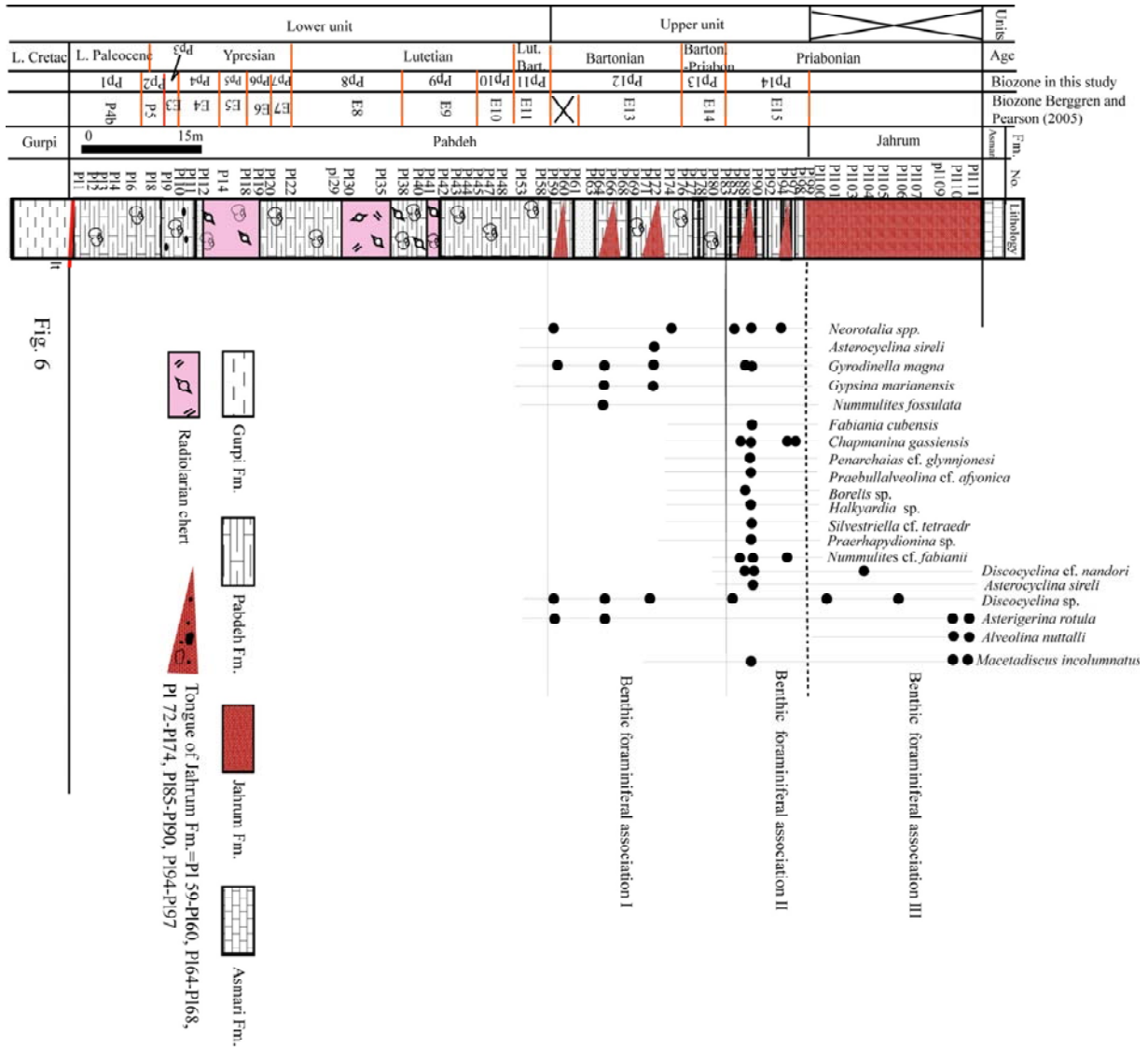


Fig. 4B





Time (Ma)	Epoch		Planktonic biozones	Berggren and Pearson (2005)	Planktonic biozones	Planktonic / benthic biozones in this study	Shallow benthic zone (SBZ) Serra-Kiel et al (1998)							
31	E. Oligocene	Rupelian	P19	<i>Turborotalia ampliapertura</i> IZ	O2	<i>Turborotalia ampliapertura</i> HOZ								
32			P18	<i>Chilouembelina cubensis-Pseudohastigerina</i> spp. IZ	O1	<i>Pseudohastigerina naguwichiensis</i> HOZ								
33	Late Eocene	Priabonian	P17	<i>Turborotalia cerroazulensis</i> IZ	E16	<i>Hantkenina alabamensis</i> HOZ	Benthic assemblage zone III Benthic assemblage zone II							
34			P16	<i>Turborotalia cunialensis/Cr. inflata</i> CRZ	E15	<i>Globigerinatheka index</i> HOZ								
35			P15	<i>Po. semiinvoluta</i> IZ	E14	<i>Globigerinatheka semiinvoluta</i> HOZ		Pb15	<i>Globigerinatheka index</i> PRZ					
36								Pb14	<i>Cribohantkenina inflata-Globigerinatheka mexicana</i> IRZ					
37	Middle Eocene	Bartonian	P14	<i>Turborotalia rohri-M. spinulosa</i> PRZ	E13	<i>Morozovella crassata</i> HOZ	Pb13	<i>M. crassata-Gl. kugleri</i> IRZ						
38									P13	<i>Globigerinatheka beckmanni</i> TRZ	E12	<i>Orbulinoides beckmanni</i> TRZ	Pb12	Benthic assemblage zone I
39			P12	<i>Morozovella lehneri</i> PRZ	E11	<i>Morozovella lehneri</i> PRZ	Pb11	<i>Morozovella lehneri</i> PRZ						
40									E10	<i>Acarinina topilensis</i> PRZ	Pb10	<i>Acarinina topilensis</i> PRZ		
41	Lutetian	P11	<i>Globigerinatheka kugleri/Morozovella aragonensis</i> CRZ	E9	<i>Globigerinatheka kugleri/Morozovella aragonensis</i> CRZ	Pb9	<i>Globigerinatheka kugleri/Morozovella aragonensis</i> CRZ							
42								P10	<i>Hantkenina nuttalli</i> IZ	E8	<i>Guembeltrioides nuttalli</i> LOZ	Pb8	<i>Gu. nuttalli-Globigerinatheka kugleri</i> IRZ	
43														P9
44	Early Eocene	P8	<i>Morozovella aragonensis</i> PRZ	E6	<i>Ac. pentacamerata</i> PRZ	Pb6	<i>Ac. pentacamerata-P. palmerae</i> IRZ							
45								P7	<i>Morozovella aragonensis/M. formosa</i> CRZ	E5	<i>Morozovella aragonensis/M. subbotinae</i> CRZ	Pb5	<i>Gu. lozanoi-Ac. pentacamerata</i> IRZ	
46														P6
47								a	<i>Morozovella velascoensis-M. formosa/M. lensiformis</i> ISZ	E3	<i>M. marginodentata</i> PRZ	Pb3	<i>M. marginodentata/M. formosa</i> IRZ	
48	Paleocene	Thamnetian	P5	<i>Morozovella velascoensis</i> IZ	E2	<i>P. wilcoxensis-M. velascoensis</i> CRZ	Pb2	<i>Morozovella velascoensis</i> PRZ						
49									P4c	<i>Ac. soldadoensis-Gl. pseudomenardii</i> ISZ	E1	<i>A. sibaiyaensis</i> LOZ	P5	<i>Morozovella velascoensis</i> IZ
50														
51	P4a	<i>Gl. pseudomenardii-Ac. subsphaerica</i> CRSZ	P4b	<i>Ac. subsphaerica</i> PRSZ	Pb1	<i>Acarinina subsphaerica</i> TZ								
52							SBZ 2 - 4							
53							SBZ 5 - 12							
54							SBZ 13 - 16							
55							SBZ 17 - 18							
56							SBZ 19 - 20							

Fig. 7